AMERICAN JOURNAL OF PHYSICAL ANTHROPOLOGY 107:273–283 (1998)

A Simple Method for Visualization of Influential Landmarks When Using Euclidean Distance Matrix Analysis

THEODORE M. COLE III,[1]* AND JOAN T. RICHTSMEIER[2]
[1]*Department of Basic Medical Science, School of Medicine, University of Missouri-Kansas City, Kansas City, Missouri*
[2]*Department of Cell Biology & Anatomy, The Johns Hopkins University Schoolof Medicine, Baltimore, Maryland*

KEY WORDS EDMA; morphometrics; landmark coordinate data

ABSTRACT Euclidean distance matrix analysis (EDMA) differs from most other morphometric methods for the analysis of landmark coordinate data in that it is coordinate-system invariant. However, strict adherence to coordinate-system invariance (for both biological and statistical reasons) introduces some difficulty in using graphic aids for the analysis and interpretation of EDMA results. We present a simple and effective graphic method to help localize important differences in form, growth, or shape by identifying "influential" landmarks. Examples are presented using simulated data and real data involving both children with craniofacial dysmorphologies and sexual dimorphism in adult *Macaca fascicularis*. Am J Phys Anthropol 107:273–283, 1998.

Euclidean distance matrix analysis (EDMA) is a method for comparing the forms or shapes of organisms that have been measured using the two- or three-dimensional coordinates of homologous anatomical landmarks (Lele and Richtsmeier, 1991; Lele, 1993). While there are a number of morphometric methods available for analyzing this type of data (see reviews by Rohlf, 1990; Richtsmeier et al., 1992; Rohlf and Marcus, 1993), EDMA is unusual in that it provides descriptions of form and shape that are coordinate-system invariant. In other words, EDMA descriptions of size and shape do not depend on the arbitrary choice of a coordinate system, and they do not change in the presence of nuisance parameters, such as translation, rotation, or reflection (Lele, 1993). EDMA comparisons of form, growth, and shape also have this invariance property. The concept of invariance, and its importance to the biologically meaningful interpretation of morphometrics, is discussed more thoroughly by Lele and Richtsmeier (1990) and by Lele (1991, 1993; Lele and McCulloch, 1998). EDMA also provides a number of important statistical advantages, including consistent (= correct) estimation of mean forms, form differences, and the variances of and covariances among landmarks (Lele, 1993; Lele and McCulloch, 1998).[1]

One notable characteristic of some previously published EDMA studies is that graphics have not played a large part in analysis and interpretation. Difficulties in displaying

[1]Other coordinate-system invariant methods include Rao and Suryawanshi's (1996, 1998) adaptations of EDMA methods and analyses of angles, the truss method (Strauss and Bookstein, 1982), and finite-element scaling analysis (Cheverud et al., 1983; Vogl, 1992). We prefer EDMA and related methods because: 1) the truss requires an a priori choice of a subset of the distances analyzed by EDMA that may not include the distances where the most important differences in form, shape, or growth occur (Lele, 1991); and 2) the results of finite-element scaling analysis are affected by an a priori choice of element design (Richtsmeier et al., 1990), which we consider to be biologically arbitrary at least to some degree.

Grant sponsor: NSF; Grant number: DBS 9209083; Grant sponsor: Project II of NIH; Grant number: 1 P50 DE11131-03.

*Correspondence to: Theodore M. Cole III, Ph.D., Department of Basic Medical Science, School of Medicine, University of Missouri-Kansas City, 2411 Holmes St., Kansas City, MO 64108. E-mail: tcole@cctr.umkc.edu

Received 7 May 1997; accepted 15 July 1998.

EDMA results are actually related to the coordinate-system-invariant properties that make EDMA biologically and statistically advantageous. Other landmark-based methods prominently feature graphic aids to interpretation. However, in making comparisons of form or shape most other landmark-based methods (e.g., shape coordinates (Bookstein, 1986), thin-plate splines and relative warps (Bookstein, 1991; Rohlf et al., 1996), or Procrustes superimposition (Rohlf and Slice, 1990)) *must* depend either on superimposition in an arbitrary, user-defined coordinate system or on arbitrarily defined loss or deformation functions (Lele, 1991, 1993; Lele and McCulloch, 1998; contra Rohlf and Marcus, 1993; contra Lynch et al., 1996). As a consequence, the biological interpretations resulting from these methods may vary according to the coordinate system chosen (Cheverud and Richtsmeier, 1986; Lele, 1991, 1993; Richtsmeier et al., 1992; Walker, 1996: Tables 1 and 2; Lele and McCulloch, 1998). Furthermore, under all but the most restrictive conditions superimposition methods have been proven to yield incorrect estimates of biologically important parameters, including mean form, mean shape, and the variances and covariances among landmarks (Lele, 1993; Lele and McCulloch, 1998). Therefore, while the appeal of graphics-oriented morphometrics is undeniable (and the temptation to superimpose is often great), we need to emphasize that graphics are of little use if they lead the investigator to make incorrect inferences.

Given the problems with many existing morphometric methods, our best alternative is to develop graphic methods within a framework that explicitly recognizes the importance of coordinate-system invariance. The purpose of this report is to present a simple graphic method for quickly identifying "influential" landmarks when using EDMA. Influential landmarks are those that make the greatest contributions to significant differences in the forms, shapes, or growth patterns of different samples (Lele and Richtsmeier, 1992). Therefore, they are of considerable interest in comparative studies. Other EDMA-based methods for localization, such as identification of the extreme elements of form- or growth-difference matrices (Lele and Richtsmeier, 1992) or computation of marginal confidence intervals for matrix elements (Lele and Richtsmeier, 1995; Lele and Cole, 1996), also offer the potential for effectively identifying influential landmarks. However, the exploratory method described here has the advantage of being less computer-intensive and tedious. It may also be applied in comparisons involving single specimens (e.g., fossils) or samples that are too small for reliable estimation of confidence intervals.

EDMA BASICS

The method for visualization of form, growth, and shape differences will be most clearly understood if some basics of EDMA are briefly reviewed. This is not intended to be a thorough discussion; readers are referred to the original citations for more complete theoretical and computational details.

Suppose an organism, called A, has been measured by recording the positions of K homologous landmarks in two- or three-dimensional space. The *form* (size and shape) of A can be completely and unambiguously described by a *form matrix* called $\mathbf{FM}(A)$:

$$\mathbf{FM}(A) = \begin{bmatrix} 0 & d(1,2) & \cdots & d(1,K) \\ d(2,1) & 0 & & \vdots \\ \vdots & & \ddots & d(K-1,K) \\ d(K,1) & \cdots & d(K,K-1) & 0 \end{bmatrix}$$

where $d(i, j)$ is the Euclidean distance between landmarks i and j. This representation of form is invariant to arbitrary translations, rotations, and reflections (Lele, 1991). For a sample of specimens, a mean form matrix can be computed following an algorithm developed by Lele (1993; Lele and Cole, 1996).

Mean forms can be used in a variety of applications, including comparisons of form (Lele and Richtsmeier, 1991), growth (Richtsmeier and Lele, 1993), or shape (Lele and Cole, 1996). For comparing the mean forms of two samples A and B (for example, sexes or species), a *form difference matrix* (Lele and Richtsmeier, 1991), called $\mathbf{FDM}(A, B)$, is calculated as follows:

$$\mathbf{FDM}(A, B)_{ij} = \frac{\mathbf{FM}(A)_{ij}}{\mathbf{FM}(B)_{ij}}$$

for $i, j = 1 \ldots K$, with the convention that $0/0 = 0$ for the diagonal elements. Each element of the **FDM** is simply the ratio of the distance between landmarks i and j in A to the same distance in B. If the forms of A and B are identical, then the off-diagonal elements of the form-difference matrix will all equal 1.0. If the shapes (proportions) of A and B are the same, but their sizes are different, the off-diagonal elements will all equal some positive scalar c, where $c \neq 1$. If the off-diagonal elements are heterogeneous, a difference in shape is indicated. Lele and Richtsmeier (1991) describe a procedure for testing the significance of form differences between two samples.

Richtsmeier and Lele (1993) have described a method of comparing growth patterns over a given developmental interval. Suppose *A1* and *A2* are samples of taxon *A* at ages 1 and 2, respectively. A *growth matrix* for *A* over that interval is defined as follows:

$$\mathbf{GM}(A1 \rightarrow A2)_{ij} = \frac{\mathbf{FM}(A2)_{ij}}{\mathbf{FM}(A1)_{ij}}$$

If a comparable growth matrix is defined for sample *B* over the same interval, a *growth difference matrix* can be used to compare relative growth patterns:

$$\mathbf{GDM}(A1 \rightarrow A2\text{: } B1 \rightarrow B2)_{ij} = \frac{\mathbf{GM}(A1 \rightarrow A2)_{ij}}{\mathbf{GM}(B1 \rightarrow B2)_{ij}} = \frac{\mathbf{FM}(A2)_{ij}/\mathbf{FM}(A1)_{ij}}{\mathbf{FM}(B2)_{ij}/\mathbf{FM}(B1)_{ij}}$$

A method for testing for significant differences in sample growth patterns was presented by Richtsmeier and Lele (1993).

Finally, Lele and Cole (1996) introduced a method for comparing the mean *shapes* of two samples. Suppose that sample *A* has a form matrix **FM**(A) and a scaling factor c_A that can be defined as a measure of the average "size" of organisms in the sample. The scaling factor is defined a priori on biological grounds. Some possible scaling factors (among others) are any single inter-landmark distance, the geometric mean of all distances, the median distance, or the maximum distance. A *shape matrix* for *A* can be defined as follows:

$$\mathbf{SM}(A)_{ij} = \frac{\mathbf{FM}(A)_{ij}}{c_A}$$

In other words, the **SM** results when each element of the **FM** is divided by the same scaling factor c_A. For comparing the mean shapes of samples *A* and *B*, a *shape difference matrix* is defined:

$$\mathbf{SDM}(A, B)_{ij} = \mathbf{SM}(A)_{ij} - \mathbf{SM}(B)_{ij}$$

Note that this last comparison is explicitly made using element-wise *differences*, not ratios. If two samples have identical mean shapes, the off-diagonals of the **SDM** will all equal zero. Otherwise, there will be non-zero off-diagonals. Lele and Cole (1996) describe a procedure for testing for significant differences in both shape and size.

IDENTIFYING INFLUENTIAL LANDMARKS USING MATRICES

Lele and Richtsmeier (1992) provided the following method for recognizing influential landmarks when examining form-difference matrices. They recommend placing the $K(K-1)/2$ off-diagonal elements into a rank-ordered column vector. Examining the extremes of the ranked vector should indicate which distances (and, by extension, which landmarks) make the greatest contributions to overall form differences. However, Lele and Richtsmeier (1992:61) note that:

> We stress that the researcher must take the time to carefully review a **FDM** in its entirety. The strength of our proposed method lies in its ability to look at all linear distances simultaneously. The temptation to look at only the extremes of the **FDM** or at predetermined regions of interest is great, but is only a useful exercise after evaluation of the entire **FDM**.

While the importance of examining the **FDM** in detail is unchanged, the method proposed here represents efforts to make exploratory EDMA studies less time-consuming and tedious. After exploratory analysis, more computer-intensive, confirmatory tests for landmark influence (Lele and Richtsmeier, 1992) may be carried out as appropriate.

A NEW VISUALIZATION METHOD

We propose a new method for using graphics to interpret EDMA results, without sacri-

ficing any of EDMA's advantages. The method is characterized by a high "data-to-ink ratio" (Tufte, 1993), so that very large amounts of information can be displayed in a clear and compact manner. The method involves a two-dimensional scatterplot, where positions on the horizontal axis correspond to the *K* landmarks (i.e., landmarks are labeled with integers from 1 to *K*). Positions along the vertical axis are real numbers corresponding to values of the off-diagonal elements of the EDMA matrix under study (**FDM**, **GDM**, or **SDM**). Each of the landmarks studied is the endpoint of *K*-1 linear distances, and at each position on the horizontal axis, the $K - 1$ matrix elements associated with the corresponding landmark (i.e., having that landmark as an endpoint) are plotted. Since EDMA matrices are symmetric, each off-diagonal matrix element will appear twice on the plot, once for each of the landmarks that define the corresponding distance.

The distribution of a single landmark's matrix elements gives a visual impression of its influence. An influential landmark may be indicated in one of two ways. First, an influential landmark might be identified by a large spread of element values, which correspond to matrix elements that lie toward both extremes of the sorted off-diagonals. Alternatively, the distribution of an influential landmark's elements might be strongly skewed, indicating matrix elements that lie to one extreme of the sorted off-diagonals, but not the other. The nature of the pattern is dependent on the geometry of the landmark configurations, as explained below.

SIMPLE EXAMPLES

Suppose that two objects are compared, each described in two dimensions by 25 landmarks. The landmarks for Object *A* are arranged in a square grid, with equal spacing along the vertical and horizontal axes (Fig. 1A). Object *B* is very similar to *A* for all of the landmarks but one, Landmark 13, which lies near the center of the object (Fig. 1B). For *B*, Landmark 13 is shifted to the right, while the vertical-axis location is unchanged. *B*'s other landmarks differ from *A*'s only by very small, random perturbations. Because the perturbation in Landmark 13 is so much greater than those in the other landmarks, it can be considered "influential" because it is the greatest source of the overall form difference between *A* and *B*. A form-difference matrix **FDM**(*B*, *A*) was calculated, and the elements are plotted in Figure 2A. In this case, the greater influence of Landmark 13 is indicated by greater dispersion of the elements corresponding to distances that have it as an endpoint. Since Landmark 13 shifts to the right, distances to the right of its position are decreased, relative to the same distances in *A*. In contrast, distances between Landmark 13 and landmarks to its left are increased, relative to the same distances in *A*. The influence of Landmark 13 is seen more clearly when distinctive symbols are used to denote the **FDM** elements that have it as an endpoint (Fig. 2B).

Figure 3 shows an example of how change in a landmark at the periphery of the configuration produces a different picture of landmark influence. The data are produced in the same way as for Object *B*: a large deviation in one landmark and very small random perturbations in the others. However, Object *C* (Figure 1C) has the large perturbation in Landmark 25, in the upper right-hand corner. Because Landmark 25 is at the periphery and is moved away from all of the other landmarks (relative to their positions in *A*), *C* is characterized by increases in all of the distances that have Landmark 25 as an endpoint (when compared to *A*). In contrast to the first form comparison, where Landmark 13 was influential, there are no decreases in distances associated with the influential landmark. As a result, the plot (Fig. 3A) shows a distribution for Landmark-25 form differences that is markedly skewed away from the others in a positive direction. Highlighting Landmark-25 form differences with a different symbol (Fig. 3B) shows how it increases the dispersion of values associated with other landmarks.

EXAMPLES USING REAL DATA

To demonstrate the method with real data, facial form in children with syndromic cra-

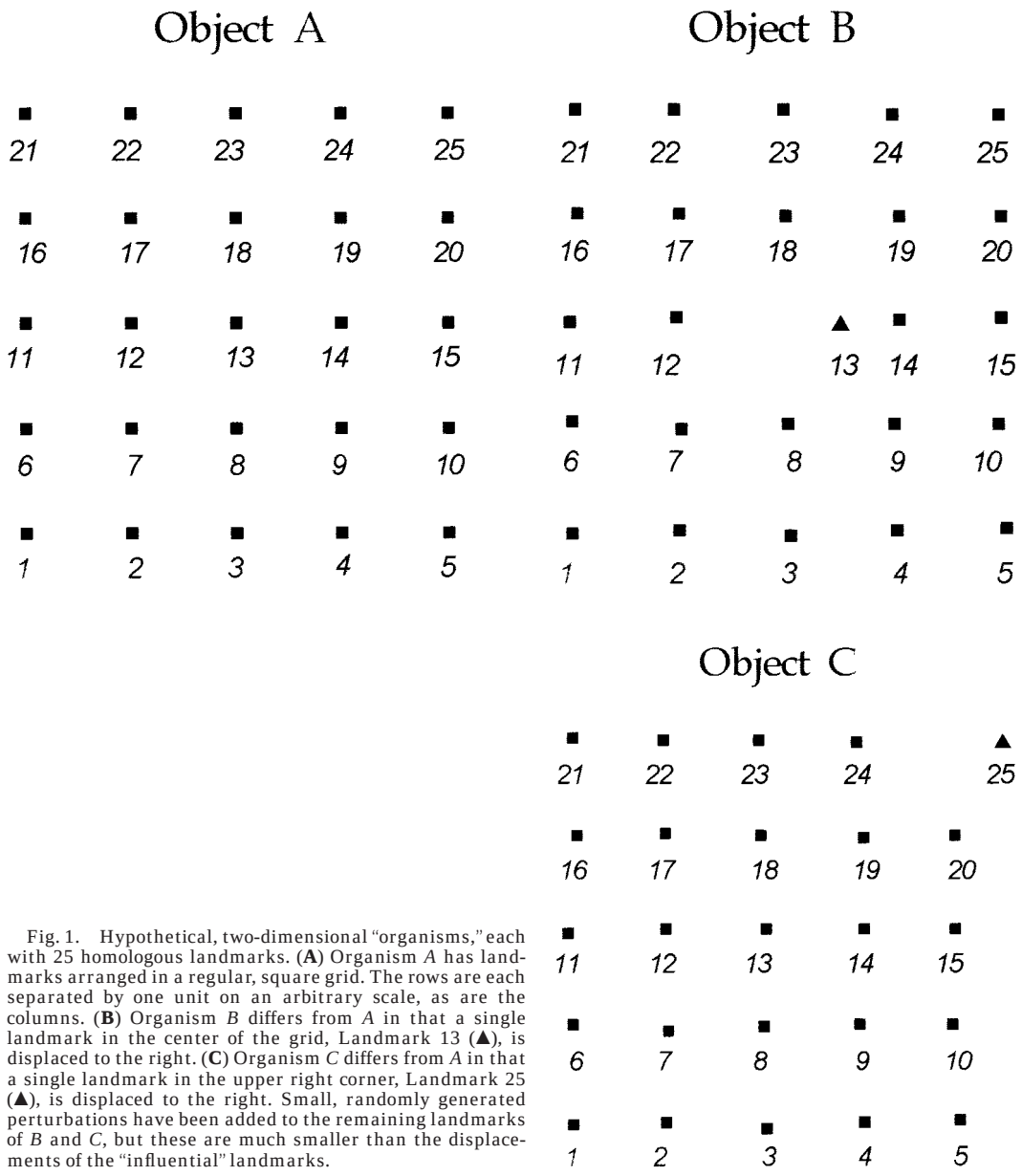

Fig. 1. Hypothetical, two-dimensional "organisms," each with 25 homologous landmarks. (**A**) Organism *A* has landmarks arranged in a regular, square grid. The rows are each separated by one unit on an arbitrary scale, as are the columns. (**B**) Organism *B* differs from *A* in that a single landmark in the center of the grid, Landmark 13 (▲), is displaced to the right. (**C**) Organism *C* differs from *A* in that a single landmark in the upper right corner, Landmark 25 (▲), is displaced to the right. Small, randomly generated perturbations have been added to the remaining landmarks of *B* and *C*, but these are much smaller than the displacements of the "influential" landmarks.

niofacial malformations was compared with form in normal children. Two-dimensional coordinates of the seven homologous landmarks (Table 1) were collected from lateral cephalograms (Richtsmeier, 1985). The landmarks are illustrated in Figure 4. Data were collected from images of normal 13-year-olds, as well as from 13-year-olds affected with either Apert syndrome or Crouzonn syndrome (Richtsmeier, 1985), and mean forms were calculated following Lele (1993). In an exploratory search for influential landmarks, form-difference matrices were calculated in separate comparisons of Apert and Crouzon samples to the normal sample. In each case, the syndromic mean form was the numerator for the **FDM**, while the normal mean form was the denominator.

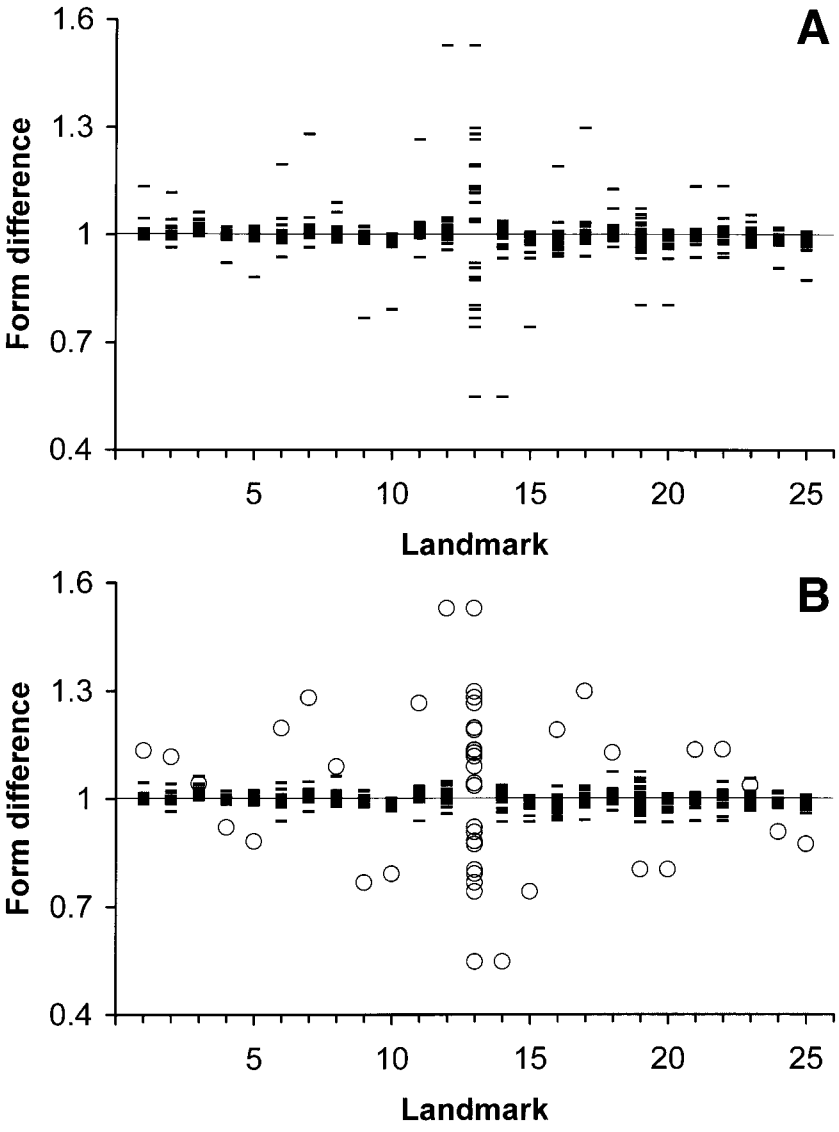

Fig. 2. Plot of the values of off-diagonal elements of **FDM** (*B, A*) on the vertical axis and landmark number on the horizontal axis. (**A**) All points are represented with identical symbols (-). Note that the greatest dispersion is associated with elements involving Landmark 13, with the dispersions for each landmark symmetrically distributed around a y-axis value of 1.0. (**B**) Elements associated with Landmark 13 have been given a distinctive symbol (○). It is now obvious that the extreme matrix values associated with each landmark are also associated with Landmark 13.

The plot for the Apert/normal comparison is presented in Figure 5A. Most of the form differences are less than 1.0, indicating that Apert patients tend to be smaller than normal (as least as indicated by the landmarks in the analysis). Landmarks 4 (intradentale—○) and 6 (sella—Δ) appear to be the most influential. The relatively large distance between Landmarks 3 (anterior nasal spine) and 4 (intradentale) in Apert patients is especially noticeable, indicated by the circles at the upper margin of the plot. While both landmarks could be described as "influential" on the basis of this *distance*, Landmark 4 (intradentale) appears to be the marginally more influential *landmark*, because form differences associated with Landmark 3 (anterior nasal spine) appear to be less variable in general. Landmark 6 (sella) also shows a fairly large degree of dispersion and is associated with the lower extremes of the distributions for Landmarks 3 (anterior

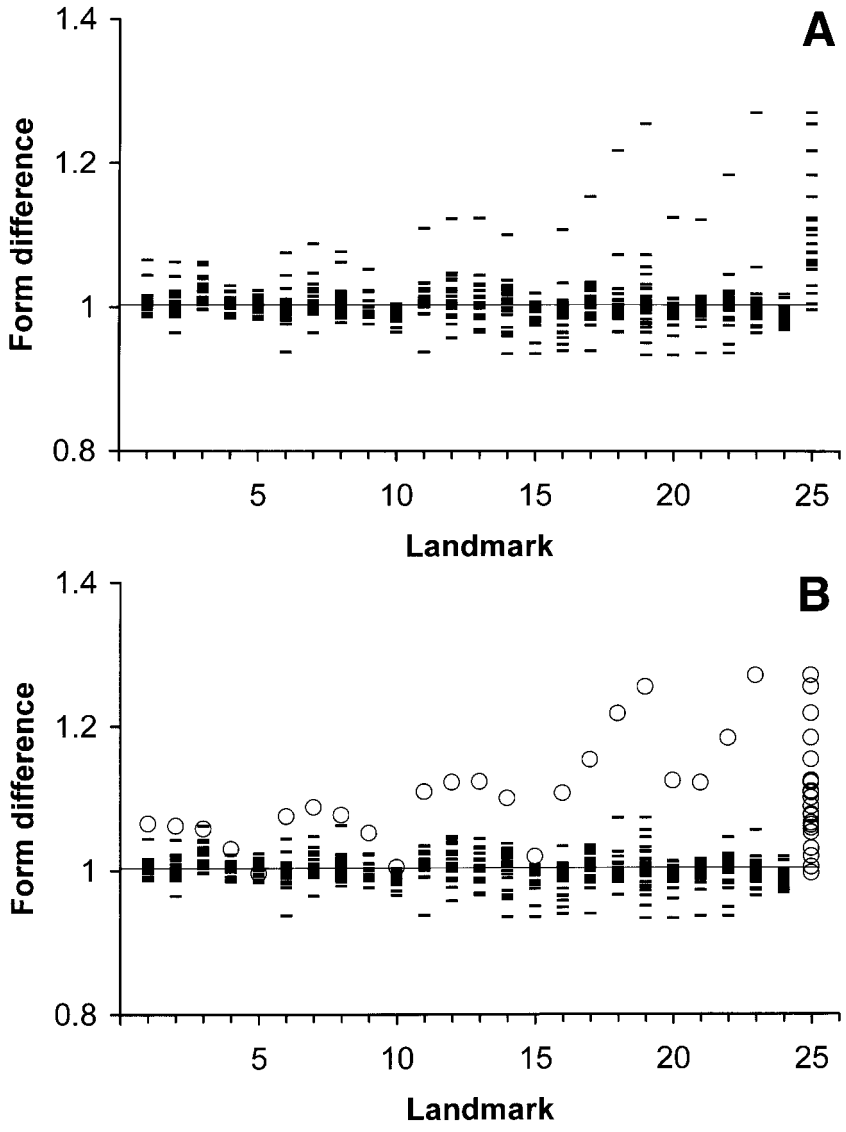

Fig. 3. Plot of the values of off-diagonal elements of **FDM**(*C, A*) on the vertical axis and landmark number on the horizontal axis. (**A**) All points are represented with identical symbols (-). Note that the greatest dispersion is associated with elements involving Landmark 25, where the y-axis values are positively skewed away from 1.0. (**B**) Elements associated with Landmark 25 have been given a distinctive symbol (○). Again, the effects of a single, influential landmark are immediately apparent.

TABLE 1. Landmarks digitized from two-dimensional cephalograms, in a comparison of normal 13-year-old males and age-matched samples of patients affected with Apert or Crouzon syndromes (see Fig. 4)

1. Nasion
2. Nasale
3. Anterior nasal spine
4. Intradentale superior
5. Posterior nasal spine
6. Sella
7. Basion

nasal spine), 5 (posterior nasal spine), and 7 (basion). A preliminary interpretation of these relatively decreased distances in Apert children is that the position of sella is more inferior than in normal children. This interpretation agrees with previous assessments of abnormal morphology of the sella turcica in Apert syndrome (Kreiborg et al., 1976; Richtsmeier, 1985, 1987, 1988).

When the Crouzon patients are compared to the normal sample, a different picture of landmark influence is seen (Fig. 5B). Here,

Fig. 4. Tracing of a lateral cephalogram of a normal child, with seven homologous landmarks (Table 1) used in comparisons between normal children and children affected with Apert or Crouzon syndromes. Modified from Richtsmeier (1988: Fig. 2).

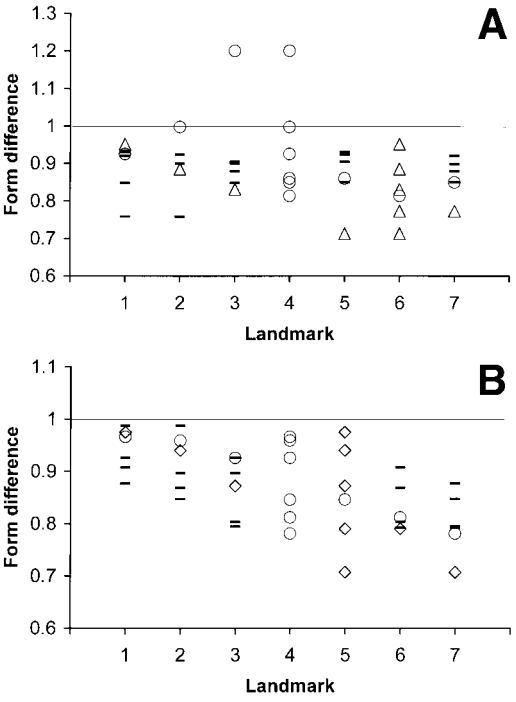

Fig. 5. (**A**) Graphic display of **FDM**(Apert, Normal). The most influential landmarks are Landmark 4 (intradentale superior—○) and Landmark 6 (sella—△). (**B**) Graphic display of **FDM**(Crouzon, Normal). The most influential landmarks are Landmark 4 (intradentale superior—○) and Landmark 5 (posterior nasal spine—◇). See text for a more thorough explanation.

all of the form differences are less than 1.0, indicating that the Crouzon 13-year-olds are smaller than their normal counterparts. For the Crouzon comparison, Landmark 5 (posterior nasal spine—◇) appears to have the greatest variation in form differences. Note that while the Landmark-5 form differences are widely dispersed, their central tendency does not differ greatly from those of other landmarks. This is probably due to the roughly central location of the posterior nasal spine within the landmark configuration (Fig. 4). Landmark 5 also appears in the most negative extremes of form distances associated with Landmarks 6 (sella) and 7 (basion), indicating that the positioning of the posterior palate (relative to the cranial base) is an important component of the difference between Crouzon and normal morphologies. Landmark 4 (intradentale—○) also appears to be fairly influential, again judging from the relatively great dispersion of distances associated with it. It is also involved in one of the more negative elements of the form-difference matrix: the distance between Landmarks 4 (intradentale) and 7 (basion). Consideration of Landmarks 4 (intradentale) and 5 (posterior nasal spine) together suggests that the position of the palate as a whole distinguishes Crouzon children from normal children. A similar morphological pattern was observed in a previous study (using finite-element scaling analysis) by Richtsmeier and Lele (1990).

As a final example, we consider sexual dimorphism in the cranium of adult *Macaca fascicularis* (Cheverud and Richtsmeier, 1986; Richtsmeier et al., 1993). The three-dimensional mean forms for adult males and females are described using 35 landmarks (Fig. 6, Table 2), and a form-difference matrix is calculated with males in the numerator. The number of elements in the form-difference matrix is 595, making a detailed analysis of the form-difference matrix tedious. However, the most influential landmarks are readily identified when plotted (Fig. 7A), where there is an upward shift in elements associated with Landmarks 9, 10, 11, and 12. These are nasale, intradentale superior, and the right and left premaxillary–maxillary junctions, respectively. The upward shift indicates that the distances associated with these landmarks are absolutely and relative larger in males. There is also a relatively large dispersion for a few

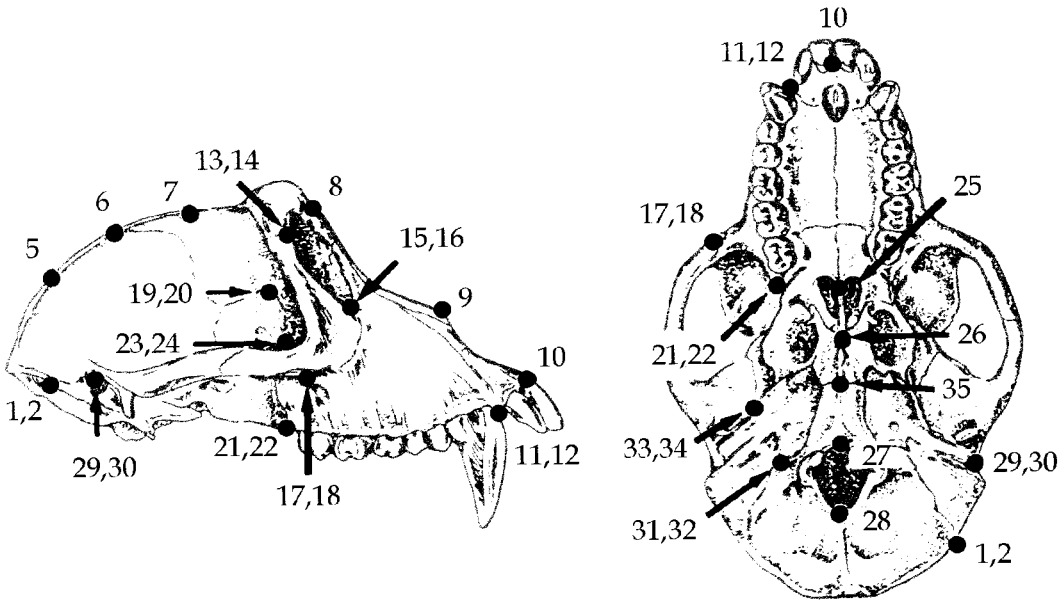

Fig. 6. Landmarks used in the three-dimensional analysis of *Macaca* sexual dimorphism (modified from Richtsmeier et al., 1993: Fig. 1). Landmark identification numbers correspond to Table 2. Bilateral landmarks are only illustrated on one side of the skull, but are labeled with numbers for both sides.

of the distances associated with Landmark 35, the midpoint of the sphenobasilar synchondrosis.

The influence of these landmarks becomes clearer when they are given distinctive symbols (Fig. 7B). Distances associated with Landmarks 9 through 12 are represented by open circles (○), while two distances associated with Landmark 35 are represented by open triangles (△). It is readily apparent that many of the most-dimorphic form differences are associated with Landmarks 9 through 12. Anatomically, these differences indicate a greater anterior projection of the premaxilla and anterior nasal opening in males, probably as a correlate of canine dimorphism. This interpretation is consistent with the findings of Richtsmeier et al. (1993). The influential status of Landmark 35 (sphenobasilar synchondrosis) indicates that there are sex differences in the anteroposterior proportions of the basicranium in the midline. The distances between Landmarks 26 (vomerosphenoid junction) and 35 are relatively larger in females, while the distance between 27 (basion) and 35 is relatively larger in males.

TABLE 2. Landmarks digitized in three dimensions, comparing cranial form in adult male and female Macaca fasicularis *(see Fig. 6)*

1. Right asterion
2. Left asterion
3. Midpoint of right asterion–bregma arc
4. Midpoint of left asterion–bregma arc
5. Midpoint of bregma–lambda arc
6. Bregma
7. Midpoint of bregma–lambda arc
8. Nasion
9. Nasale
10. Intradentale superior
11. Right premaxilla–maxilla junction (alveolus)
12. Left premaxilla–maxilla junction (alveolus)
13. Right frontozygomatic junction
14. Left frontozygomatic junction
15. Right zygomaxillare superior
16. Left zygomaxillare superior
17. Right zygomaxillare inferior
18. Left zygomaxillare inferior
19. Right pterion anterior
20. Left pterion anterior
21. Right maxillopalatine junction
22. Left maxillopalatine junction
23. Right pterygopalatine fissure
24. Left pterygopalatine fissure
25. Posterior nasal spine
26. Vomerosphenoid junction
27. Basion
28. Opisthion
29. Right external auditory meatus
30. Left external auditory meatus
31. Right jugular process
32. Left jugular process
33. Right temporosphenoid junction
34. Left temporosphenoid junction
35. Sphenobasilar synchondrosis

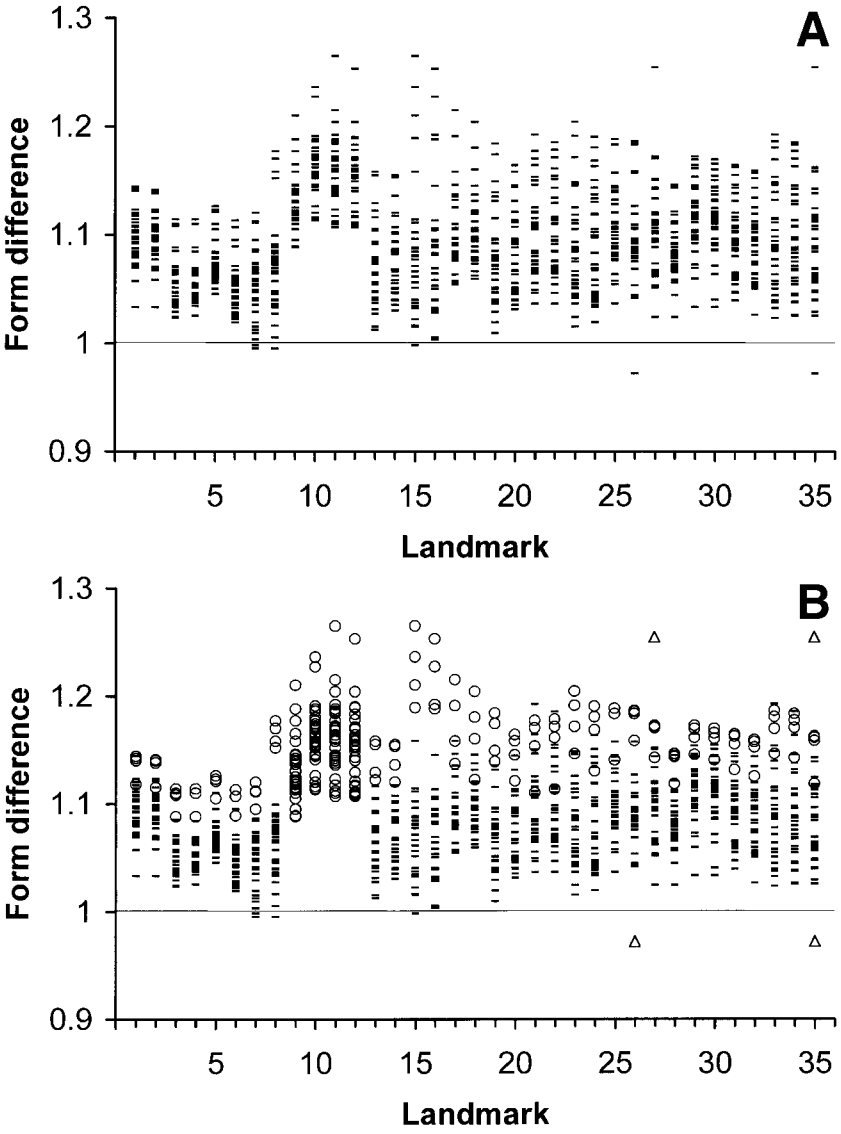

Fig. 7. Graphic display of **FDM**(*Macaca* male, *Macaca* female), where 35 landmarks are used (Table 2). (**A**) All points have identical symbols (-). Note the marked, positive skewness of elements associated with Landmarks 9, 10, 11, and 12, as well as the relatively great, symmetric dispersion of Landmarks 26, 27, and 35. (**B**) Landmarks associated with different regions of the skull have been given distinctive symbols. Those associated with the premaxilla and anterior nasal aperture (9 through 12) are denoted by ○. Note how these distances increase the upper range of the form differences associated with most other landmarks. Selected distances associated with the sphenobasilar synchondrosis are denoted by △. See text for a more thorough explanation.

NOTES ON PLOT PREPARATION

The examples above used a variety of symbols to illustrate the distributional densities and to highlight distances associated with influential landmarks. Some general recommendations can be made regarding symbol selection. Bulky, filled symbols (e.g., ■, ●, or ▲) should be avoided because points quickly become obscured when there are even a moderate number of landmarks, making details of the distributions impossible to see. Other symbols to avoid include hollow symbols with more than one horizontal component (e.g., □). In preparing this report, simple dashes (-) were found to be the most effective in presenting detailed, but clear, pictures of distributional densities. Small dots (•) can also be effective, although they may need to be "jittered" (Wilkinson, 1990) slightly for greater clarity by adding small amounts of random noise to their horizontal positions. In highlighting influential landmarks, hollow symbols without parallel horizontal components are recommended (e.g., ○ and △); Wilkinson (1990) recommends hollow circles in particular for visualizing

distributional densities. For color illustrations, additional flexibility is gained by highlighting influential matrix elements with contrasting shapes and colors.

Finally, an anonymous reviewer suggested that a clearer picture of the relative influence of landmarks could be gained through a sequential elimination of landmarks from the plot (beginning with the most influential). Such a procedure would nicely complement the "omit one" testing procedure proposed by Lele and Richtsmeier (1992). However, the investigator should be careful to preserve the horizontal and vertical scales of the plot, so that the perceptions of influence are consistent from one plot to another. Alternatively, one could produce a series of plots where each landmark was given a distinctive symbol in turn.

ACKNOWLEDGEMENTS

Thanks to Maria Cole, William Jungers, Gail Krovitz, Michael Lague, Subhash Lele, and Maureen O'Leary for their comments and constructive criticisms. We also appreciate the constructive suggestions provided by anonymous reviewers.

LITERATURE CITED

Bookstein FL (1986) Size and shape spaces for landmark data in two dimensions. Stat. Sci. *1:*181–242.

Bookstein FL (1991) Morphometric Tools for Landmark Data. New York: Cambridge University Press.

Cheverud JM, Lewis J, Lew W, and Bachrach W (1983) The measure of form and variation in form: An application of three dimensional morphology by finite element methods. Am. J. Phys. Anthropol. *61:*151–166.

Cheverud JM, and Richtsmeier JT (1986) Finite element scaling applied to sexual dimorphismin rhesus macaque (*Macaca mulatta*) facial growth. Syst. Zool. *35*:381–399.

Kreiborg S, Prydsoe U, Dahl E, and Fogh-Andersen P (1976) Calvarium and cranial base in Apert's syndrome: An autopsy report. Cleft Palate J. *13:*296–303.

Lele S (1991) Some comments on coordinate-free and scale invariant methods in morphometrics. Am. J. Phys. Anthropol. *85:*407–417.

Lele S (1993) Euclidean distance matrix analysis (EDMA): Estimation of mean form and mean form difference. Math. Geol. *25:*573–602.

Lele S, and Cole TM III (1996) A new test for shape differences when variance-covariance matrices are unequal. J. Hum. Evol. *31:*193–212.

Lele S, and McCulloch, C (1998) Invariance and morphometrics. J. Am. Stat. Assoc. Submitted.

Lele S, and Richtsmeier, JT (1990) Statistical models in morphometrics: Are they realistic? Syst. Zool. *39:* 60–69.

Lele S, and Richtsmeier, JT (1991) Euclidean distance matrix analysis: A coordinate free approach to comparing biological shapes using landmark data. Am. J. Phys. Anthropol. *86:*415–428.

Lele S, and Richtsmeier JT (1992) On comparing biological shapes: Detection of influential landmarks. Am. J. Phys. Anthropol. *87:*49–65.

Lele S, and Richtsmeier JT (1995) Euclidean distance matrix analysis: Confidence intervals for form and growth differences. Am. J. Phys. Anthropol. *98:*73–86.

Lynch JM, Wood CG, and Luboga SA (1996) Geometric morphometrics in primatology: Craniofacial variation in *Homo sapiens* and *Pan troglodytes.* Folia Primatol. *67:*15–39.

Rao CR, and Suryawanshi S (1996) Statistical analysis of shape of objects based on landmark data. Proc. Natl. Acad. Sci. USA *93:*12132–12136.

Rao CR, and Suryawanshi S (1998) Statistical analysis of shape through triangulation of landamarks: a study of sexual dimorphism in hominoids. Proc. Natl. Acad. Sci. USA *95:*4121–4125.

Richtsmeier JT (1985) A study of normal and pathological craniofacial morphology and growth using finite element methods. Ph.D. dissertation, Northwestern University.

Richtsmeier JT (1987) Comparative study of normal, Crouzon, and Apert craniofacial morphology using finite element scaling analysis. Am. J. Phys. Anthropol. *74:*473–493.

Richtsmeier JT (1988) Craniofacial growth in Apert syndrome as measured by finite-element scaling analysis. Acta Anat. *133:*50–56.

Richtsmeier JT, and Lele S (1990) Analysis of craniofacial growth in Crouzon syndrome using landmark data. J. Craniofac. Gen. Dev. Biol. *10:*39–62.

Richtsmeier JT, Morris GR, Marsh JL, and Vannier MW (1990) The biological implications of varying element design in finite-element scaling analyses of growth. Ann. Int. Conf. IEEE Eng. Med. Biol. Soc. *12:*387–388.

Richtsmeier JT, Cheverud JM, and Lele S (1992) Advances in anthropological morphometrics. Annu. Rev. Anthropol. *21:*283–305.

Richtsmeier JT, Cheverud JM, Danahey SE, Corner BD, and Lele S (1993) Sexual dimorphism of ontogeny in the crab-eating macaque (*Macaca fascicularis*). J. Hum. Evol. *25:*1–30.

Rohlf FJ (1990) Morphometrics. Annu. Rev. Ecol. Syst. *21:*299–316.

Rohlf FJ, and Marcus LF (1993) A revolution in morphometrics. Trends Ecol. Evol. *8:*129–132.

Rohlf FJ, and Slice DE (1990) Extensions of the Procrustes method for optimal superimposition of landmarks. Syst. Zool. *39:*40–59.

Rohlf FJ, Loy A, and Corti M (1996) Morphometric analysis of Old World Talpidae (Mammalia, Insectivora) using partial-warp scores. Syst. Biol. *45:*344–362.

Strauss RE, and Bookstein FL (1982) The truss: Body form reconstructions in morphometrics. Syst. Zool. *31:*113–115.

Tufte ER (1993) The Visual Display of Quantitative Information. Cheshire, CT: Graphics Press.

Vogl C (1992) Theoretical enhancements of finite-element scaling analysis (FESA) methodology. Syst. Biol. *42:*341–355.

Walker JA (1996) Principal components of shape variation within an endemic radiation of threespine stickleback. In LF Marcus, M Corti, A Loy, GJP Naylor, and DE Slice (eds.): Advances in Morphometrics. NATO ASI Series A, Volume 284. New York: Plenum, pp. 321–334.

Wilkinson L (1990) SYGRAPH: The System for Graphics. Evanston, IL: Systat, Inc.